

# A synergistic approach of the application of SiO<sub>2</sub> Nanoparticles and Ionic Liquid in Enhanced Oil Recovery

Prasenjit Talukdar<sup>a\*</sup>, Jiban Saikia<sup>b</sup>, Mitu Das<sup>a</sup>, Abhai Giri<sup>a</sup>,  
Mousum Gogoi<sup>a</sup>, Himashish Kalita<sup>a</sup>, Biki Boruah<sup>a</sup>, Gaurav Himanta  
Khaklari<sup>c</sup>

<sup>a</sup>Department of Petroleum Engineering, DUIET, Dibrugarh University, Assam, 786004, India

<sup>b</sup>Department of Chemistry, Dibrugarh University, Assam, 786004, India

<sup>c</sup>Department of Petroleum Technology, Dibrugarh University, Assam, 786004, India

\*Corresponding author's email address: [prasenjit\\_duiet@dibru.ac.in](mailto:prasenjit_duiet@dibru.ac.in)

The increasing demand for enhanced oil recovery (EOR) techniques has led to active research in cost-effective and environmental sustainability. This work, examines the possibility of synergistic effects between silicon dioxide nanoparticles (SiO<sub>2</sub> NPs) and ionic liquids in EOR - in terms of interfacial tension reduction, contact angle modification, and enhancing fluid mobility. Key experimental results indicate that the addition of SiO<sub>2</sub> nanoparticles to alkali-surfactant-polymer (ASP) solutions significantly lowers IFT and increases viscosity, both of which are key to improving oil displacement efficiency. The addition of ionic liquid [C16 mim]<sup>+</sup>Br<sup>-</sup> further optimizes interfacial properties, achieving ultra-low IFT of 0.0000681 mN/m and promoting oil recovery under extreme reservoir conditions. These results demonstrate the capability of SiO<sub>2</sub> nanoparticles to stabilize emulsions and ionic liquids in reducing surfactant adsorption, thus offering a robust and innovative chemical EOR strategy. Although promising laboratory results are reported, the cost, scalability, and stability of the nanoparticles have to be addressed for field applications. This work emphasizes the use of nanotechnology and ionic liquids to develop new, efficient, and sustainable petroleum recovery techniques.

**Keywords:** Nanoparticles, Ionic Liquid, Interfacial Tension, Wettability, Thermal Stability, Enhanced Oil Recovery.

## 1. Introduction

The fluctuations in prices in the oil industry have led to the need to adopt cheap techniques of EOR. In the past, the main techniques used for modifying IFT and enhancing the wettability of reservoir rocks and the sweep efficiency are based on the use of surfactants, alkalis, and polymers. However, their relatively high costs and environmental impacts have compelled researchers to seek for environmentally friendly solvents such as ionic liquids. As possessing properties of molten salts, ionic liquids have advantages of high thermal stability, flame retardancy, and wide solubility, thus being ideal surface-active agents. The alkyl chain

modified ionic liquids can effectively lower the IFT and adjust the wettability of carbonate rock, and the effectiveness can still be maintained in high salinity and high-temperature conditions. The use of deep eutectic solvents (DES) based ionic liquids has been tested in experiments, which gave high, up to 0.2 mN/m of water-oil interfacial tension reduction and a great enhancement in oil recovery factors as shown by Y. Zhou et al. (2020) [1]. Other applications include the use of polymers in EOR to reduce viscous fingering and improve sweep efficiency through the management of fluid displacement, as highlighted by K. S. Sorbie (2013) and X. LU et al. (2012) [2][3]. It has been evidenced from some field application that they are effective [4][5][6][7]. Surfactants that are both hydrophilic and lipophilic decrease IFT while the high gas content forms high viscosity foams leading to enhanced sweep efficiency [8]. Water injection, especially when using low-salinity water, has been deemed efficient for EOR [9][10]. Furthermore, the improvement in the nanotechnology has proved that nanoparticles could improve the rate of oil recovery through the following ways and interactions[11].

Among the various processes that are triggered by nanoparticles in EOR, the most critical one is wettability alteration [12][13][14]. There are certain conditions and restrictions associated with the process of EOR, which nanotechnology can alleviate. Although, there are still some ambiguous findings, a significant number of tests and field applications in different parts of the world substantiate the effectiveness of nanoparticles in EOR [15][16][15][17].

Ionic liquids are potential candidates for combating the problems associated with the use of surfactants in EOR because they can modify the wettability of the reservoir rocks and reduce the IFT of the oil-water system. It is better in extreme reservoir conditions than surfactants because they demonstrate more stability. The interfacial tension can be reduced to  $10^{-2}$  mN/m and may increase the oil recovery factor by 15% using ionic liquids. However, the ASP flooding which is an improvement of the alkaline-surfactant flooding has its own challenges such as alkali deposition and formation erosion. The use of weak alkaline ASP chemicals with SiO<sub>2</sub> nanoparticles is a new method of EOR with enhanced interaction and efficiency in controlling the fluid mobility, flow visualization of emulsions, lower interfacial tension and wettability alteration.

Among all types of nanoparticles, silicon dioxide (SiO<sub>2</sub>) nanoparticles are of great interest for EOR. They can modify its wettability, lower its interfacial tension, regulate mobility of fluids and enhance the reservoir conformity. SiO<sub>2</sub> nanoparticles are thermally and chemically stable with other EOR methods and can be applied to fracturing. Such characteristics render SiO<sub>2</sub> nanoparticles suitable for increasing oil recovery in a range of reservoir environments. This article concentrates on the use of nanoparticles in the techniques of EOR. It explores key factors, classifications of nanoparticles, ways to control the stability of nanofluids. As for the environmental issues and the nanoparticle synthesis, they are not discussed in the present paper, but may be considered in further research works.

## **2. Material and Methods**

Different components used for formulation of the required EOR slug have been tabulated in the Table 1. Moreover, a number of equipments have been used in this study. A Specific Gravity Apparatus determines fluid density, while a Digital Weighing Balance ensures precise chemical measurements. A Probe Sonicator disperses the nanoparticles evenly in fluids, and a Spinning Drop Tensiometer measures interfacial tension between oil and water. The MCR

72 Rheometer assesses fluid rheological parameters under various conditions, and a Magnetic Spinner Mixer ensures thorough mixing of solutions, all contributing to accurate and reliable EOR experiment.

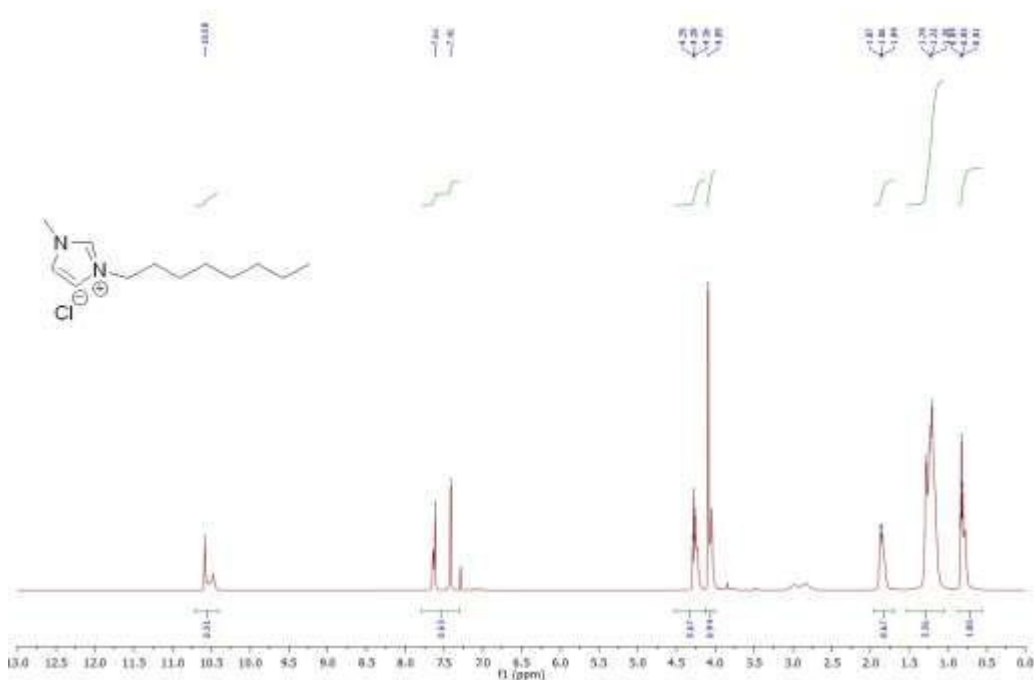
**Table 1: Name and Specifications of the components used in this study**

Name of component	Compound	Uses	Specifications
Ionic liquid	[C <sub>16</sub> mim] <sup>+</sup> Br <sup>-</sup> 1-hexadecyl-3-methylimidazolium bromide	To reduce IFT between oil and water, sometimes increase viscosity, High thermal and chemical stability	Molecular Weight-387.44 CAS No. : 132361-22-9 Purity : 98% Melting point: 42.0°C
Polymers	Carboxymethyl Cellulose (CMC)	To improve the efficiency of oil recovery processes	pH (1% solution)-6.5-8.0 Viscosity (2% in water; 20°C)-400 - 800 cps
Surfactants	Cetyl Trimethyl Ammonium Bromide (CTAB)	Reduce IFT and wettability alteration	Molar mass (M) 364,46 g/mol Density (D) 0,5 g/cm <sup>3</sup> Melting point (mp) 243 °C
Alkali	Sodium Carbonate (Na <sub>2</sub> CO <sub>3</sub> )	Produce insitu surfactant to reduce IFT between l-aqueous and oleic phase	Molecular weight - 105.99 Chloride (Cl):0.01% Sulphate (SO <sub>4</sub> ):0.02% Iron (Fe):0.002% Heavy Metals (Pb):0.002%
Nanoparticles	Silicon Dioxide (SiO <sub>2</sub> )	Ability to reduce the interfacial tension (IFT) between oil and water, profile control and displacement efficiency after water flooding, ASP + SiO <sub>2</sub> nanoparticles mixture forms strong viscoelastic, thermodynamic, and kinetic stability of the droplets, thereby	Boiling point -2230 °C (1013 hPa) Density-2.56 g/cm <sup>3</sup> not applicable Melting Point-1713 °C pH value-3.7 - 4.7

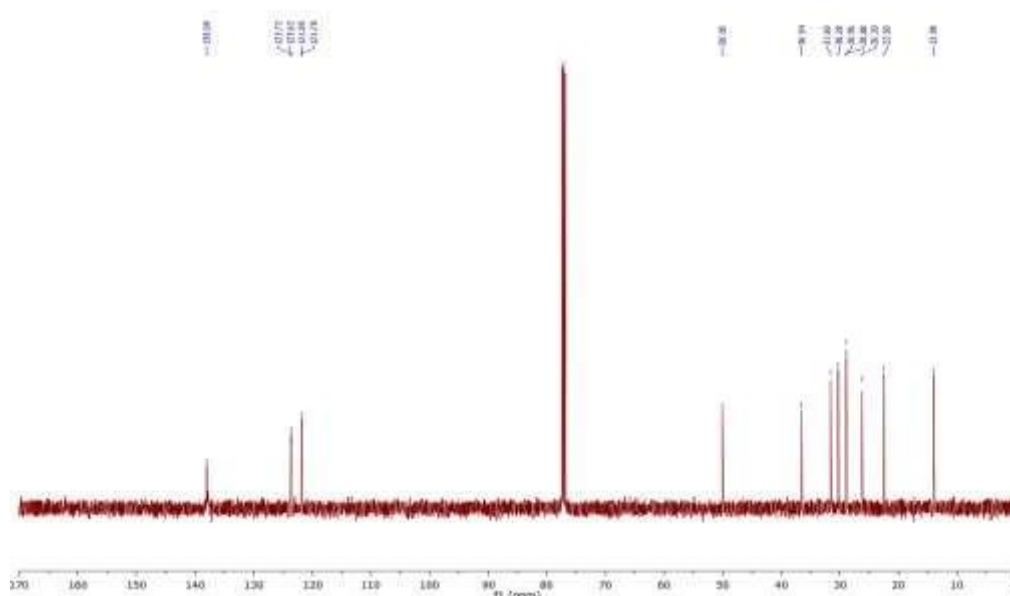
		resulting in a larger sweep efficiency and better displacement efficiency	
--	--	---------------------------------------------------------------------------	--

## 2.1. NMR spectroscopy

In  $^1\text{H}$  NMR, or hydrogen NMR spectroscopy, one can observe the magnetic properties of hydrogen nuclei-protons within a molecule. This methodology is utilized in identifying particular unique chemical environments of hydrogen atoms, from which it states their surroundings and how they interact with neighboring atoms. Structure, bonding, as well as functional groups in organic compounds, are thus highlighted by the features of chemical shifts, signal splitting, and coupling patterns observed in  $^1\text{H}$  NMR. This is useful in the delineation of structural differences and molecular arrangements. Carbon-13 NMR, or  $^{13}\text{C}$  NMR spectroscopy, is based on carbon-13 nuclei - one of the less abundant isotopes of carbon, providing extensive structural information. In  $^{13}\text{C}$  NMR, carbon atoms of different chemical environments are signaled uniquely, so it provides valuable information about the carbon skeleton of a molecule. Having lower sensitivity than  $^1\text{H}$  NMR due to the low natural abundance of  $^{13}\text{C}$ , it is still an important method for establishing kinds and connectivity of carbon atoms and, therefore, forms a convenient adjunct tool to hydrogen NMR for organic structure elucidation. Fig. 1(a) and (b) shows the  $^1\text{H}$  NMR and  $^{13}\text{C}$  NMR with their detailed specifications for the Ionic Liquid used in this study.



(a)  $^1\text{H}$  NMR (500 MHz,  $\text{CDCl}_3$ )  $\delta$  10.58 (s, 1H), 7.61-7.41 (d,  $J = 99.3$  Hz, 2H), 4.29 (t,  $J = 7.4$  Hz, 2H), 4.09 (s, 3H), 1.87 – 1.84 (m, 2H), 1.24 – 1.20 (m, 10H), 0.84 (t,  $J = 6.9$  Hz, 3H).



(b) <sup>13</sup>C NMR (125 MHz, CDCl<sub>3</sub>) δ 138.00, 123.67, 121.82, 50.05, 36.54, 31.60, 30.28, 28.92, 26.20, 22.50, 13.98.

**Fig. 1:** (a) <sup>1</sup>H spectra of [MPIM][HCOO] and (b) <sup>13</sup>C spectra of [MPIM][HCOO]

### 3. Experimental Work and Results

The Spinning Drop Tensiometer was used to calculate the interfacial tension (IFT) of the samples while rheological properties were measured with Rheometer Model MCR-72. The IFT was determined using the following equation with the help of Spinning Drop Tensiometer.

$$\gamma = 1.44 \times 10^{-7} (\Delta P; D^3) (\theta^2) \text{-----} (1)$$

Where,  $\gamma$  = IFT, mN/m

$\Delta P$  = Density difference brine-oil in g/cc

$D$  = Diameter in mm read directly from instrument

$\theta$  = Rotation in rpm read directly from instrument

EOR is positively impacted by reduced IFT as it reduces the capillary forces that hold the oil in the reservoir and allows for easier movement in the porous formation. Furthermore, the change in IFT can also cause the wettability of the reservoir rocks to shift from oil-wet to water-wet which in turn improves the efficiency of oil displacement and recovery. In water flooding, the IFT values of 1 to 10 mN/m are normally desired to enhance the oil displacement without forming a high amount of emulsion. For the surfactant-polymer based EOR, the IFT values are lowered to the range of 0.001 to 0.1 mN/m, while ultra-low IFT of about 0.001 mN/m greatly improves the rate of oil mobilization and recovery.

#### 3.1. Preparation of Polymer and Alkali Solutions

Synthesis of polymer and alkali solutions is an integral part of formulation of enhanced oil recovery (EOR) fluids. The preparation of Carboxymethyl Cellulose (CMC) polymer solutions step-by-step followed by their sodium carbonate (Na<sub>2</sub>CO<sub>3</sub>) modification in the

following subsections is shown to be crucial in optimizing them for rheology as well as reduction of interfacial tension (IFT) in order to increase oil displacement efficiency.

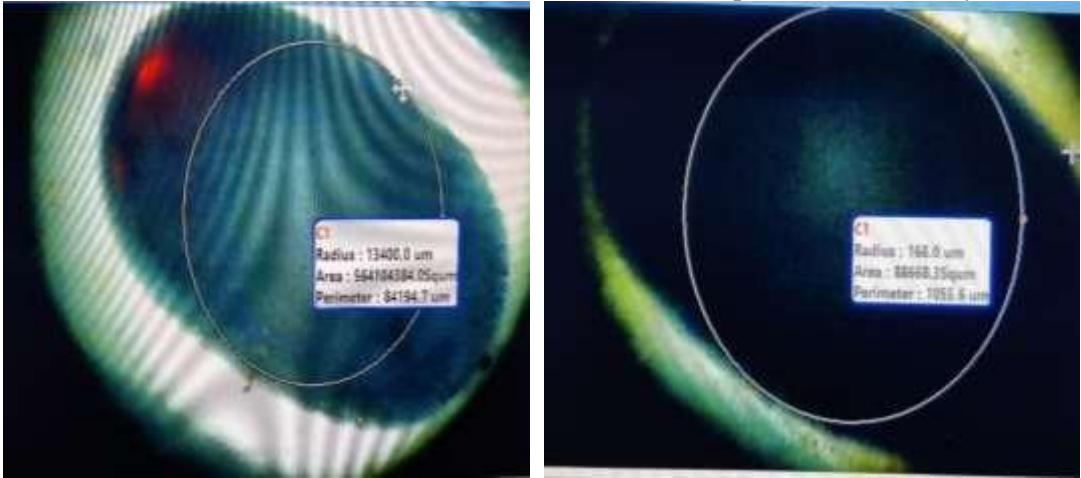
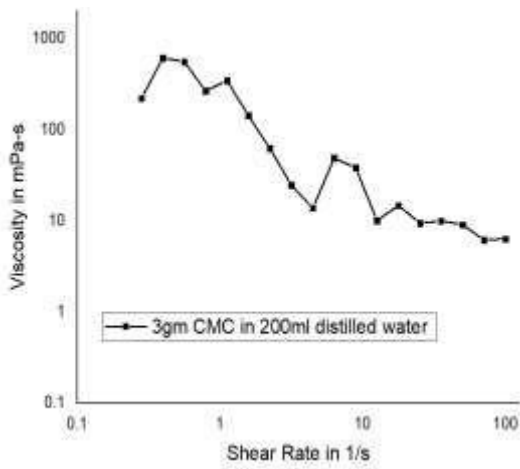
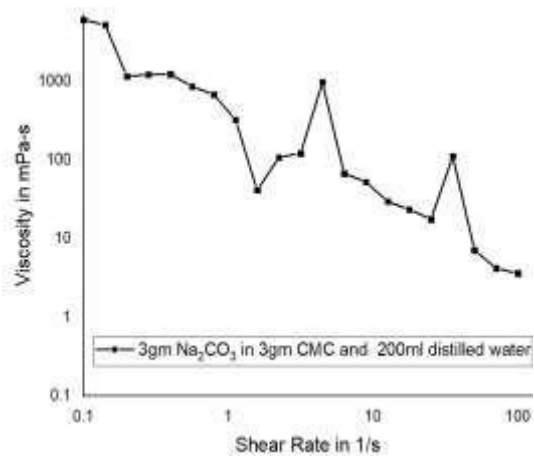


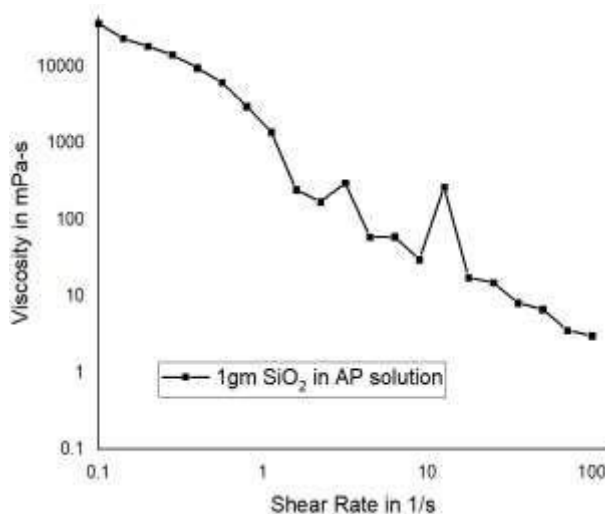
**Figure 1: IFT measurement for (A) Alkali ( $\text{Na}_2\text{CO}_3$ ) in Polymer (CMC) solution and (B) ( $\text{SiO}_2$ ) added to AP Solution**



(a)



(b)



(c)

**Figure 2: Viscosity vs Shear Rate Graph for (a) 3gm CMC; (b) Alkali ( $\text{Na}_2\text{CO}_3$ ) in Polymer (CMC) solution and (c) ( $\text{SiO}_2$ ) added to the AP Solution**

### 3.1.1. Carboxymethyl Cellulose (CMC) Polymer Solution

Polymer solution was formulated by dissolving 3 grams of Carboxymethyl Cellulose (CMC) into 200 milliliters of distilled water under a magnetic stirrer and probe sonicator for proper dispersion. The solution was stirred consistently until it reached total homogenization. The prepared solution density was measured with a specific gravity apparatus and was 1.01738  $\text{g/cm}^3$ . The viscosity was also measured with a mud balance and was 8.5 ppg. The rheological behavior of the solution was also studied, and the viscosity vs. shear rate curve (Figure 2(a)) was plotted to determine its flow characteristics.

### 3.1.2. Alkali ( $\text{Na}_2\text{CO}_3$ ) in CMC Solution

To analyze the influence of an alkali on the polymer solution, 3 grams of sodium carbonate ( $\text{Na}_2\text{CO}_3$ ) was mixed with the already prepared CMC solution (200 mL). The mixture was continuously stirred and ultrasonically treated with a probe sonicator to achieve a uniform dispersion. The density of the obtained alkali-polymer (AP) solution was determined with a specific gravity apparatus and was found to be 1.02741  $\text{g/cm}^3$ . The viscosity, as measured by a mud balance, was constant at 8.53 ppg. The IFT was measured with a Spinning Drop Tensiometer, and a captured photograph (Figure 1(A)) illustrates the measurement process. The IFT measured was 13.4 mN/m. The viscosity vs. shear rate plot (Figure 2(b)) was examined to assess the rheological stability of the solution.

### 3.1.3. $\text{SiO}_2$ Nanoparticles in Alkali-Polymer (AP) Solution

Using a sonicator and magnetic mixing equipment, 1 gram of  $\text{SiO}_2$  nanoparticles was added to a pre-made AP solution for this experiment. The density was then determined using a specific gravity device. Figure 1(B) shows the picture captured from the Spinning Drop Tensiometer for the measurement of interfacial tension, and Figure 2(c) presents the viscosity vs. shear rate graph for this sample. The estimated IFT was found to be  $13.63 \times$



$10^{-3}$  mN/m. The density of the modified solution was  $1.027871 \text{ g/cm}^3$ , and the viscosity, measured using a mud balance, remained at 8.5 ppg.

### 3.2. Surfactant-based Formulations

#### 3.2.1. Surfactant (CTAB) Solution (1.5%)

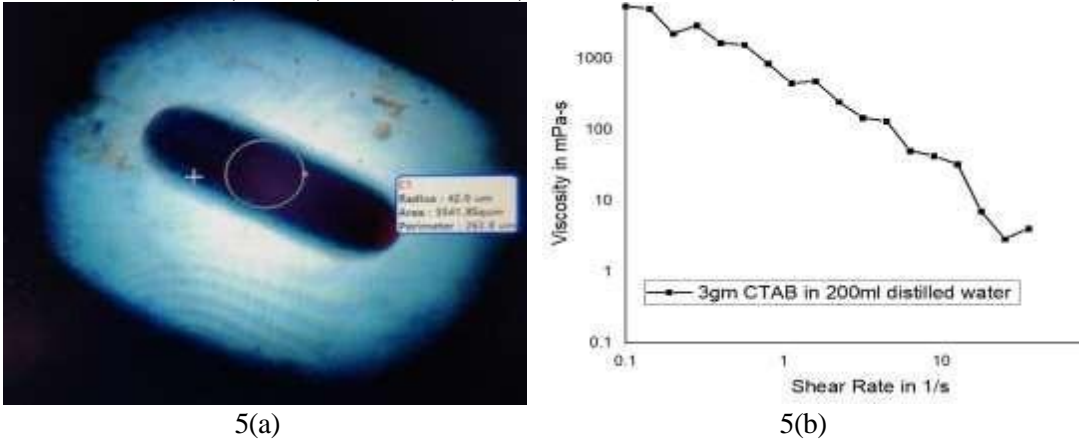


**Figure 3: (a) Picture for IFT measurement and (b) Viscosity vs Shear Rate of Surfactant solution of 1.5%**

In this experiment, 200ml of distilled water is mixed with 3g of CTAB using a magnetic mixture and a probe sonicator. The density of the combination is then determined using a specific gravity apparatus. Fig. 5 (a) shows the picture captured from the Spinning Drop Tensiometer for the measurement of the interfacial tension and Fig. 5 (b) shows the viscosity vs shear rate graph for this sample. Measured IFT is  $0.695 \times 10^{-3}$  mN/m. The density is found to be  $1.01035 \text{ gm/cm}^3$  and viscosity is measured by using mud balance and found to be 8.5ppg.

#### 3.2.2. Surfactant + Polymer (SP) Solution

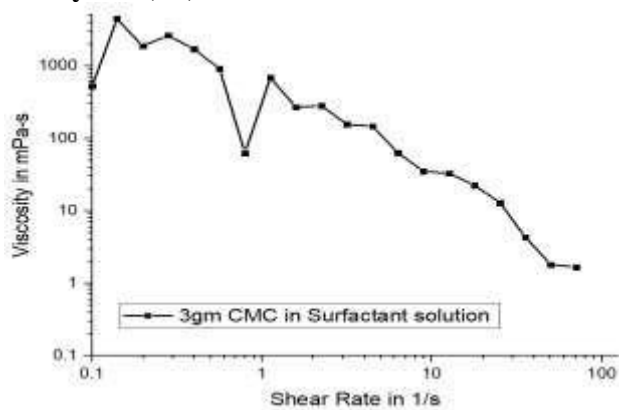


**Figure 4: Viscosity vs Shear rate of Surfactant (CTAB) + Polymer (CMC) Solution**

Using a sonicator and magnetic mixing equipment, 3 grams of CMC is added to a pre-made

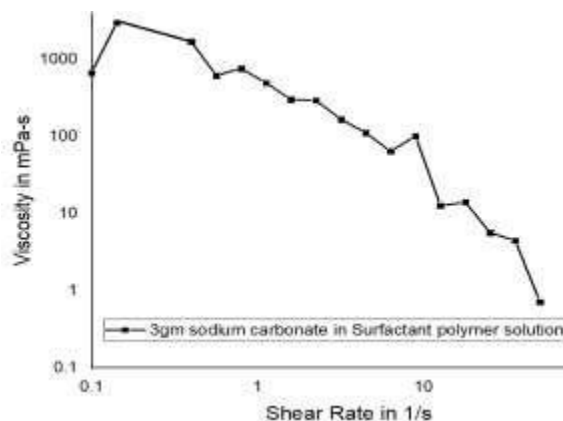


surfactant solution for this experiment. The density is then determined using a specific gravity device. Fig. 6 shows the viscosity vs shear rate graph for this sample. The density is found to be  $1 \text{ gm/cm}^3$  and viscosity is measured by using mud balance and found to be 8.53 ppg.

### 3.2.3. Surfactant + Polymer + Alkali (SPA) Solution



7(a)



7(b)

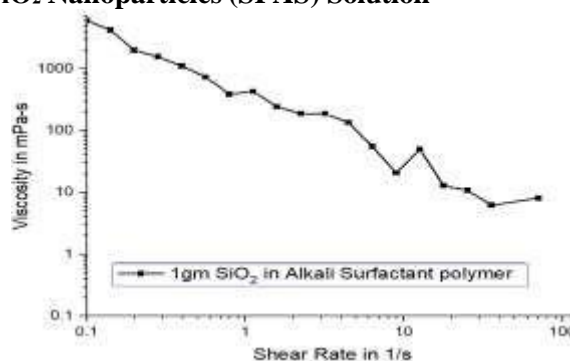
**Figure 4: (a) Picture for IFT measurement and (b) Viscosity vs Shear Rate of Surfactant (CTAB) + Polymer (CMC) Solution + Alkali ( $\text{Na}_2\text{CO}_3$ )**

In this experiment, 3 grams of sodium carbonate are added to a previously made solution of surfactant polymer, and the mixture is thoroughly mixed using a sonicator and magnetic mixing apparatus. The density is then measured using the specific gravity apparatus. Fig. 7 (a) shows the picture captured from the Spinning Drop Tensiometer for the measurement of the interfacial tension and Fig. 7 (b) shows the viscosity vs shear rate graph for this sample. Determined IFT is  $0.11017 \text{ mN/m}$ . The density is found to be  $1.02868 \text{ gm/cm}^3$  and viscosity is measured.

### 3.2.4. Surfactant + Polymer + Alkali + $\text{SiO}_2$ Nanoparticles (SPAS) Solution



8(a)



8(b)

**Figure 5: (a) Picture for IFT measurement and (b) Viscosity vs Shear rate of Surfactant (CTAB) + Polymer (CMC) + Alkali ( $\text{Na}_2\text{CO}_3$ ) +  $\text{SiO}_2$  (Nanoparticles) Solution**

In this experiment, a sonicator and magnetic mixing apparatus are used to mix the produced alkali surfactant polymer solution with 1 gram of  $\text{SiO}_2$ . A device that measures specific gravity is then used to determine the density. Fig. 8 (a) shows the picture captured from the Spinning Drop Tensiometer for the measurement of the interfacial tension and Fig. 8 (b) shows the viscosity vs shear rate graph for this sample. Estimated IFT is 0.0000681 mN/m. The density is found to be 1.03196  $\text{gm}/\text{cm}^3$  and viscosity is measured.

### 3.2.5. Final Solution: SPAS + Ionic Liquid ([C16mim]Br)

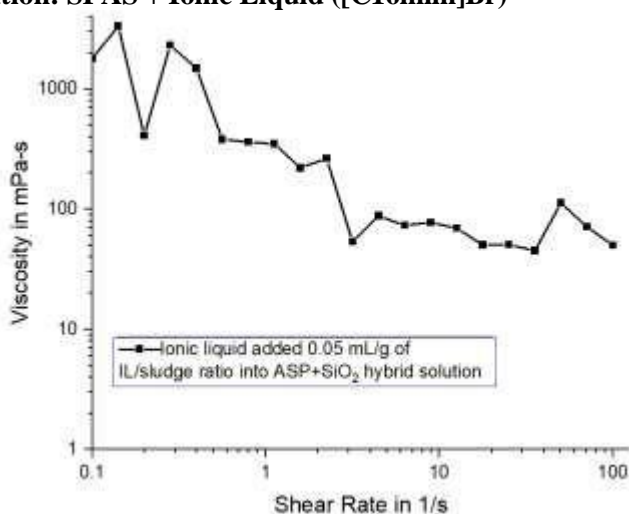


**Figure 6: Viscosity vs Shear rate of Surfactant (CTAB) + Polymer (CMC) + Alkali ( $\text{Na}_2\text{CO}_3$ ) +  $\text{SiO}_2$ (Nanoparticles) + Ionic Liquid [C16 mim] + Br-Solution**

Using a sonicator and magnetic mixing equipment, 0.05 mL/g of ionic liquid is added to the previously prepared ASP +  $\text{SiO}_2$  hybrid solution. The density is then determined using specific gravity equipment. Fig. 9 shows the viscosity vs shear rate graph for this sample. The density is found to be 1  $\text{gm}/\text{cm}^3$  and viscosity is measured.

## 4. Conclusion

This work exhibits the potential synergism between  $\text{SiO}_2$  nanoparticles and ionic liquids in EOR. The key finding here is that  $\text{SiO}_2$  nanoparticles blended with ASP solutions decrease the IFT of the solution and increase the viscosity, both of which are important factors for oil displacement efficiency. Notably, the addition of ionic liquid [C16 mim] $^+$ Br $^-$  to the ASP +  $\text{SiO}_2$  hybrid solution further improved interfacial properties, achieving an exceptionally low IFT of 0.0000681 mN/m, indicating enhanced oil displacement efficiency. The combined approach effectively alters rock wettability, reduces surfactant adsorption, and stabilizes the emulsion flow, thereby optimising oil recovery under reservoir conditions. However, the promising outcomes need to consider challenges such as cost, scalability, and stability of

nanoparticle dispersions toward field-scale applications. In general, the synergistic exploitation of SiO<sub>2</sub> nanoparticles and ionic liquids constitutes a quite robust and innovative strategy in chemical EOR, with potential to greatly increase the efficiency of oil recovery, as well as open up pathways towards more sustainable and economical exploitation of petroleum resources. Such future research should include optimization of large-scale production, cost reduction, and establishing the interactions between nanoparticles and ionic liquids and the impact of reservoir conditions to ensure realistic application.

### **Acknowledgment**

The authors wish to thank Dibrugarh University's Department of Petroleum Engineering, Department of Petroleum Technology, and Department of Petroleum Engineering for granting them access to the institutional facilities and resources necessary to complete the work, without which it would not have been feasible.

### **REFERENCES**

- [1] Y. Zhou et al., "Polymer nanoparticles based nano-fluid for enhanced oil recovery at harsh formation conditions," *Fuel*, vol. 267, no. January, 2020, doi: 10.1016/j.fuel.2020.117251.
- [2] K. S. Sorbie, *Polymer-Improved Oil Recovery*. Springer Netherlands, 2013.
- [3] X. LU et al., "Enhanced oil recovery mechanisms of polymer flooding in a heterogeneous oil reservoir," *Pet. Explor. Dev.*, vol. 48, no. 1, pp. 169–178, 2021, doi: 10.1016/S1876-3804(21)60013-7.
- [4] D.-M. Wang, J.-C. Cheng, J.-Z. Wu, and G. Wang, "Application of polymer flooding technology in Daqing Oilfield," vol. 26, pp. 74–78, Jan. 2005.
- [5] M. Han, W. Xiang, J. Zhang, W. Jiang, and F. Sun, "Application of EOR technology by means of polymer flooding in Bohai Oil fields," *Int. Oil Gas Conf. Exhib. China 2006 - Sustain. Growth oil Gas*, vol. 2, pp. 1078–1083, 2006, doi: 10.2523/104432-ms.
- [6] S. Mishra, A. Bera, and A. Mandal, "Effect of Polymer Adsorption on Permeability Reduction in Enhanced Oil Recovery," *J. Pet. Eng.*, vol. 2014, pp. 1–9, 2014, doi: 10.1155/2014/395857.
- [7] X. Wang et al., "A metal-free polymeric photocatalyst for hydrogen production from water under visible light," *Nat. Mater.*, vol. 8, no. 1, pp. 76–80, 2009, doi: 10.1038/nmat2317.
- [8] S. M. Hosseini-Nasab, M. Taal, and P. L. J. Zitha, "Effect of Newtonian and Non-Newtonian Viscosifying Agents on the Stability of Foam for EOR - Part I, under Bulk Condition," *IOR 2017 - 19th Eur. Symp. Improv. Oil Recover.*, no. April, 2017, doi: 10.3997/2214-4609.201702312.
- [9] S. Han, M. Yoo, D. Kim, and J. Wee, "Carbon Dioxide Capture Using Calcium Hydroxide Aqueous Solution as the Absorbent," pp. 3825–3834, 2011.
- [10] Z. Zhao et al., "A new kind of nanohybrid poly(tetradecyl methyl-acrylate)-graphene oxide as pour point depressant to evaluate the cold flow properties and exhaust gas emissions of diesel fuels," *Fuel*, vol. 216, no. June 2017, pp. 818–825, 2018, doi: 10.1016/j.fuel.2017.07.087.
- [11] C. A. Franco, C. A. Franco, R. D. Zabala, Í. Bahamón, Á. Forero, and F. B. Cortés, "Field Applications of Nanotechnology in the Oil and Gas Industry: Recent Advances and Perspectives," *Energy & Fuels*, vol. 35, no. 23, pp. 19266–19287, Dec. 2021, doi: 10.1021/acs.energyfuels.1c02614.
- [12] Y. Li et al., "Achieving the Super Gas-Wetting Alteration by Functionalized Nano-Silica for Improving Fluid Flowing Capacity in Gas Condensate Reservoirs," *ACS Appl. Mater. Interfaces*, vol. 13, no. 9, pp. 10996–11006, 2021, doi: 10.1021/acsami.0c22831.
- [13] T. Huang, B. A. Evans, J. B. Crews, and C. K. Belcher, "Field case study on formation fines

- control with nanoparticles in offshore wells,” *Proc. - SPE Annu. Tech. Conf. Exhib.*, vol. 5, no. 1991, pp. 3952–3959, 2010, doi: 10.2118/135088-ms.
- [14] Y. Kaito, A. Goto, D. Ito, S. Murakami, H. Kitagawa, and T. Ohori, “First Nanoparticle-Based EOR Nano-EOR Project in Japan: Laboratory Experiments for a Field Pilot Test,” *SPE Improved Oil Recovery Conference*. p. D011S008R001, Apr. 25, 2022, doi: 10.2118/209467-MS.
- [15] C. Lyu, Z. Ligu, Z. Ning, M. Chen, and D. Cole, “Review on Underlying Mechanisms of Low Salinity Waterflooding: Comparisons between Sandstone and Carbonate,” *Energy & Fuels*, vol. 36, Feb. 2022, doi: 10.1021/acs.energyfuels.1c04248.
- [16] L. Li, X. Guo, D. H. Adamson, B. A. Pethica, J. S. Huang, and R. K. Prudhomme, “Flow improvement of waxy oils by modulating long-chain paraffin crystallization with comb polymers: An observation by X-ray diffraction,” *Ind. Eng. Chem. Res.*, vol. 50, no. 1, pp. 316–321, 2011, doi: 10.1021/ie101575w.
- [17] M. Y. Kanj, M. H. Rashid, and E. P. Giannelis, “Industry first field trial of reservoir nanoagents,” *SPE Middle East Oil Gas Show Conf. MEOS, Proc.*, vol. 3, no. September, pp. 1883–1892, 2011, doi: 10.2118/142592-ms.